Published in final edited form as:
Anal Biochem. 2008 March 15; 374(2): 386–395. doi:10.1016/j.ab.2007.11.002.

Site-directed circular dichroism of proteins: ^1L_b bands of Trp resolve position-specific features in tear lipocalin

Oktay K. Gasymov, **Adil R. Abduragimov**, and **Ben J. Glasgow***
Departments of Pathology and Ophthalmology, UCLA School of Medicine, Los Angeles, CA, 90095

Abstract

The absorption spectra of *N*-acetyl-L-tryptophanamide in various solvents were resolved into the sums of the ^1L_a and ^1L_b components. The relative intensities of the 0-0 transitions of the ^1L_b bands correlate linearly with the solvent polarity values (E_T^N). A novel strategy, which utilizes a set of the experimental ^1L_b bands, was employed to resolve the near-UV CD spectra of tryptophanyl residues. Resolved spectral parameters from the single-tryptophan mutants of tear lipocalin (TL), F99W and Y87W, corroborate the fluorescence as well as structural data of TL. Analysis of the ^1L_b bands of the Trp CD spectra in proteins is a valuable tool to obtain the local features. The "DMSO-like" ^1L_b band of Trp CD spectra may be used as a "fingerprint" to identify the tryptophanyl side chains in situations where the benzene rings of Trp have van der Waals interactions with the side chains of its nearest neighbor. In addition, the signs and intensities of the components hold information about the side-chain conformations and dynamics in proteins. Combined with Trp mutagenesis, this method we call site-directed circular dichroism is broadly applicable to various proteins to obtain the position-specific data.

Keywords

tear lipocalin; Lipocalin-1; von Ebner's gland protein; Trp; vibronic band; circular dichroism; near-UV CD; site-directed circular dichroism

Introduction

Trp fluorescence is highly sensitive to the local environment of its side chain. Advances made in Trp photophysics have revealed the local features (such as polarity, proximity of quenching groups, etc) of proteins that effect quantum yield, λ_{max} and lifetime distribution of the fluorescence [1–6]. Trp has become a reliable chromophore (label) for studies of the structure-function relationship of the proteins. The solution structure of human tear lipocalin (TL), has been resolved with site-directed tryptophan fluorescence (SDTF) [7] and, later, verified by x-ray crystallography [8]. Trp is also utilized extensively by other spectroscopic techniques, such as absorption and circular dichroism (CD) spectroscopies [9,10].

The side chain of Trp possesses unique features that make CD spectroscopy valuable as a tool for the studies of the conformations of proteins. In proteins, Trp fluorescence almost

*Corresponding Author-Ben J. Glasgow, 100 Stein Plaza Rm. B-279, Los Angeles, CA 90095, Fax (310) 794-2144, Phone (310) 825-6998, E mail-bglasgow@mednet.ucla.edu.

exclusively originates form the excited electronic state ^1L_a [5,11]. However, the near-UV CD spectra of Trp residues of proteins reflect both the ^1L_a and ^1L_b electronic transitions. The intensities and signs of the CD spectra for these transitions vary independently. As a result, the near-UV CD spectra of Trp, representing the sums of various types of overlapping ^1L_a and ^1L_b bands, are very complex. The indole moiety of Trp is inherently optically inactive. A variety of mechanisms that may induce the near-UV CD bands have been implicated for aromatic side chains [12]. The interaction of the Trp side chain with another aromatic side chain (His, Tyr, Trp, Phe) or with amide groups within about 10 Å may give appreciable CD intensity [12]. The spatial arrangement of these groups in the protein determines the sign and intensity of the CD band. Therefore, the near-UV CD spectra of proteins reflect the conformation of the protein. In contrast, the nearest environment of the indole ring has the most impact on the quantum yield and lifetime distribution of Trp fluorescence [2,13].

Previously, a few attempts have been made to resolve the near-UV CD spectra of Trp by fitting the spectra to the sum of the ^1L_a and ^1L_b components [14,15]. It has been shown that one type of the ^1L_b spectrum is not sufficient for the fitting of certain types of tryptopan CD spectra. Some success has been achieved in resolving the near-UV CD spectra of Trp by varying the relative intensity of the 0-0 transition of ^1L_b in the fitting procedure. Relative intensities of vibronic bands of ^1L_b vary for Trp in buffer compared with that included in a protein structure [14]. The ^1L_b transition, in contrast to the ^1L_a, is quite sensitive to the methyl or methoxy substitutions on the indole ring, particularly at positions 4, 6, and 7. This results in changes of the relative intensities of the vibronic transitions [5,16]. It is reasonable to expect similar effects, although much smaller in scale, for Trp in instances where its benzene ring interacts with other side chains. Therefore, it is rational that various types of the ^1L_b bands would be required for the spectral fitting of the near-UV spectra of Trp included in protein structures. The λ_{max} of the ^1L_a band is much more sensitive to the environment compared with that of the ^1L_b. However, because of the high degree of inhomogeneous broadening, the vibronic bands of the ^1L_a are not resolved. In addition, for all observed ^1L_a spectra, the maximum of the absorption appears far from the 0-0 transition [5]. Accordingly, in proteins, the overall spectral shift of one kind of ^1L_a band is likely to be adequate for the spectral fitting of the near-UV CD spectra of Trp. The challenge is to provide the experimental basis to resolve various types of the ^1L_b bands that can be linked to the local features of proteins.

In this paper, we describe a novel strategy for the resolution of the near-UV CD spectra of tryptophanyl residues into the ^1L_a and ^1L_b components. That is, instead of variation of the relative intensity of the 0-0 transition in ^1L_b [15], an experimental set of the ^1L_b bands were obtained from the absorption spectra of *N*-Acetyl-L-tryptophanamide (NATA) in various solvents for the fitting procedure. As a result, the number of variable parameters is reduced. In addition, the ^1L_b band that best fits the near-UV CD spectrum of Trp located at a particular site of the protein can be linked to the particular solvent and, therefore, to the local polarity of the environment of the Trp side chain. The sensitivity of the spectral parameter ($^1L_b(0\text{-}0)/^1L_b(0\text{+}850)$) to the environment makes the ^1L_b band very attractive for protein studies.

Here we show that analysis of the ^1L_b bands of the Trp CD spectra in proteins provides the site-specific information in the proteins. The “DMSO-like” ^1L_b band of Trp CD spectra may be used as a “fingerprint” to identify specific tryptophanyl side chains in which the benzene rings of Trp has van der Waals interactions with the side chains of its nearest neighbor.

Materials and methods

NATA, ethanol, methanol, chloroform, and acetonitrile were purchased from Sigma-Aldrich. Dimethyl sulfoxide (DMSO) was purchased from Fisher Scientific. All solvents were spectrophotometric grade.

Site-Directed Mutagenesis and Plasmid Construction

The TL cDNA in PCR II (Invitrogen, San Diego, CA), previously synthesized [17], was used as a template to clone the TL gene spanning bases 115–592 of the previously published sequence [18] into pET 20b (Novagen). Flanking restriction sites for NdeI and BamHI were added to produce the native protein sequence as found in tears but with an initiating methionine [19]. To construct mutant proteins with a single tryptophan, the previously well characterized TL mutant, W17Y, was prepared with oligonucleotides (Universal DNA Inc.) by sequential PCR steps [20,21]. Using this mutant as a template, mutant cDNAs were constructed in which the selected amino acids were additionally substituted with tryptophan or cysteine. Amino acid 1 corresponds to His, bases 115–118 according to Redl [18]. Single-Trp mutants include W17Y/Y87W (for simplicity denoted as Y87W)) and W17Y/F99W (F99W).

Single-Cys mutants include C101L/K83C (K83C) and C101L/Y87C (Y87C).

Expression and purification of mutant proteins

The mutant plasmids were transformed in E. coli BL 21 (DE3) and cells were cultured and proteins were expressed according to the manufacturer's protocol (Novagen). Following cell lysis [22], the supernatant was treated with methanol (40% final concentration) at 4° C for 2 1/2 hours. Alternatively, mutant proteins expressed in inclusion bodies were dissolved in 8M urea at room temperature for 2 h. In either case, the resulting suspension was centrifuged at 3000g for 30 minutes. The supernatant was dialyzed against 50 mM Tris-HCl pH 8.4. First, the dialysate was treated to 45% saturation with ammonium sulfate. Then the supernatant from the precipitation was adjusted to 75% saturation with ammonium sulfate. The resulting precipitate was dissolved in 50 mM Tris-HCl pH 8.4 and applied to a Sephadex G-100 column (2.5 × 100 cm) equilibrated with 50 mM Tris-HCl, 100 mM NaCl, pH 8.4. The fraction containing the mutant protein was dialyzed against 50 mM Tris-HCl, pH 8.4 and applied to a DEAE Sephadex A-25 column. Bound protein was eluted with a 0–0.8 M NaCl gradient. Eluted fractions containing mutant proteins were centrifugally concentrated (Amicon, Centricon-10). Purity of mutant proteins was verified by SDS tricine gel electrophoresis [23]. The protein concentrations were determined by the biuret method [24].

Preparation of apo-TL

TL expressed in E. coli was considered as the holo-form. Recombinant TL is rich with palmitic acid but in contrast to native TL does not contain cholesterol [21,23].

To generate apo-TL, delipidation of recombinant TL was performed by a rigorous chloroform/methanol extraction and verified by thin layer chromatography as previously described [23].

Absorption Spectroscopy

UV absorption spectra were recorded at room temperature using Shimadzu UV-2400 PC spectrophotometer. DMSO, unlike other solvents used in this study, has relatively high absorbance at 265 nm. Therefore, Trp spectrum in DMSO was measured using a cell with pathlength of 5 mm. The maximum absorption did not exceed 1 OD.

CD Spectral Measurements

Spectra were recorded (Jasco 810 spectropolarimeter, 0.2 mm and 10 mm path lengths for far-UV and near-UV spectra, respectively) using a protein concentration of 1.2 mg/mL. Eight and sixteen scans from 190 to 260 nm and from 250 to 320 nm were averaged, respectively. Results were recorded in millidegrees and converted to molar $\Delta\varepsilon$ in $M^{-1}cm^{-1}$ and mean residue $\Delta\varepsilon_{MRV}$ for near-UV and far-UV, respectively.

Fitting of the absorption and CD spectra

The absorption spectra of NATA were measured in various solvents, the polarity values (E_T^N) of which differ greatly. The resolutions of the NATA spectra into the ^1L_a and ^1L_b components were achieved by using the fitting strategy described in detail elsewhere [15]. Briefly, the ^1L_b band of Barth et al. [14] was deconvolved into five Gaussian components. The existence of the five vibronic bands has been shown experimentally for the ^1L_b of a related model compound, 5-methoxyindole [25]. The line widths and amplitudes of the Gaussian components were varied to improve fitting of the ^1L_b band in various solvents. However, no deconvolution was necessary for the ^1L_a band of Barth et al. [14]. As a result, the set of the ^1L_b components, each of which corresponds to NATA in a particular solvent, was obtained. The near-UV CD spectra were resolved by testing all types of ^1L_b components. The goodness of fit was assessed by the χ^2 criterion.

Programs

For deconvolution of the spectra into Gaussian components, Microcal ORIGIN software (Northampton, MA) was used. Manipulation and fitting of tryptophan absorption and CD spectra were carried out using computer programs written in LabVIEW (National Instruments, Austin, TX). To obtain the best fit of the near-UV CD spectra, the software was programmed to find the best linear combination of the ^1L_b and ^1L_a bands, the remaining aromatic component (designated as the W17Y contribution), as well as a baseline component permitting the shift of the whole spectrum. For all spectra, 250 points were generated in the range of 270–320 nm with an increment of 0.2 nm. The ^1L_a and ^1L_b bands were shifted in steps of 0.2 nm. In fitting procedures, the same ^1L_a spectrum was used for the all CD spectra of the single-tryptophan mutants. However, each ^1L_b spectrum, which was resolved from the absorption spectra of NATA in various solvents, was tested to get the best-fit spectrum. To select the solvent that best characterizes the environment of Trp residue in the mutant proteins, χ^2/χ^2_{min} values were calculated for the various solvent-specific ^1L_b components.

Results and discussion

The contribution of Tyr87 to the near-UV CD spectra of TL

The aromatic composition of the W17Y mutant includes 6 tyrosines and 3 phenylalanine residues. Since phenylalanine residues contribute below 270 nm in the CD spectra, the remaining aromatic component originates from the tyrosine residues for the spectral region >270 nm. In the mutant, Y87W, there are only five tyrosines. In the fitting procedure, the intensity of the CD spectrum of W17Y was varied to compensate for the lost contribution of Tyr87 in this mutant. However, deletion of this contribution to the CD spectrum of Y87W may alter the spectral shape of the total tyrosine contribution. In this case, the CD spectra of the mutant W17Y may not be used for the total tyrosine contribution. Therefore, to justify use of W17Y in the fitting procedure, the CD spectrum of Tyr87 was examined. The spectral contribution of the Tyr87 to the CD spectrum was constructed as the difference of the CD spectra of K83C and Y87C (Fig. 1). The difference CD spectrum is very similar to that of W17Y. The difference in spectral range < 270 nm can be attributed to contribution from phenylalanine residues, which is absent in the difference CD spectrum because of cancellation

in the spectral subtraction (Fig. 1B). The CD spectra were deconvolved by fitting into sum of the spectral components in the range of 270–320 nm. Therefore, in the analysis of the CD spectrum of Y87W, it is justified to use the CD spectrum of W17Y as a variable component to compensate for the lost contribution of Tyr87. The construction of the CD spectrum of Tyr87 by use of recombinant TL instead of K83C resulted in a similar CD spectrum, but some negative inclination in the spectral region of > 290 nm (data not shown). This difference may be attributed to the slight alterations in the environment of Trp17 that affect its ^1L_a band. Perhaps, the contributions of Trp17 to the CD spectra are very similar in the mutants K83C and Y87C. As a result, the difference CD spectrum, which was constructed by using these mutants, does not show any obvious peaks from the Trp17 but there is small broad positive band greater than 290 nm in W17Y and K83C-Y87C.

Characterization of TL mutants

The far-UV CD spectrum of the TL mutant, F99W, which has been published previously [26], is very similar to that of recombinant TL. The far-UV spectrum of apoF99W is also similar to that of apo-TL and shows an expected decrease of β-structure [26,27]. It indicates that the substitution of the Phe with a Trp at position 99 does not alter the secondary structure of TL. The far-UV CD spectra of the TL mutants, K83C and Y87C, are similar to that of recombinant TL (Fig. 2). The difference CD spectrum (Y87W and Y87C) is consistent with the aromatic contribution to the far-UV CD rather than changes in secondary structure of Y87W [28,29] (Fig. 2, inset). Therefore, all mutant proteins used in this study have the native fold and contain structural information that is relevant to TL.

The absorption spectra of Trp in various solvents and their resolution into the ^1L_a and ^1L_b components

It is well documented that the absorption spectra of Trp and its derivatives are sensitive to solvent polarity and depend on the ability of a solvent to form a hydrogen bond with the NH-group of the indole moiety [30]. The near-UV absorption spectrum of Trp consists of the two overlapping ^1L_a and ^1L_b bands, for which transition moments are perpendicular to each other [5].

The near-UV absorption spectra of NATA in various solvents are shown in Figure 3; the solvent polarity values vary greatly. It is evident that the resolutions as well as positions of the vibronic bands of the absorption spectra are different from each other. The spectra were fitted as the sum of the ^1L_a and ^1L_b components using a method described previously [15]. The result of fitting and the resolution into the components are shown in Figures 3 and 4. As expected from prior published studies, the solvent-induced spectral shifts are greater for the ^1L_a band compared with those of the ^1L_b. It has been shown that the ^1L_a transition has a substantial charge transfer component and therefore a larger change in the dipole moment [5]. The ^1L_a band is therefore highly sensitive to the environment. The ^1L_a transition induces large geometry changes in the indole ring that results in a large absorption bandwidth and a low intensity for the 0-0 transition. Because of the very large number of bands, most of which are positioned more that 2000 cm^{-1} above the 0-0 transition, that have Franck-Condon factors $>10^{-4}$ times that of the 0-0 transition, the λ_{max} of the ^1L_a band is always located far from the 0-0 transition [5]. The resulting inhomogeneous broadening in the ^1L_a makes its vibronic bands almost untraceable even for the 0-0 transition.

In contrast to the transition for ^1L_a, the ^1L_b exhibits much less charge transfer and small geometry changes. As a result, compared to that of ^1L_a, the relative intensity of the 0-0 transition of the ^1L_b band is higher. The transition dipole moment of the ^1L_b is approximately perpendicular to that of the ^1L_a and its magnitude is significantly weaker [5]. However, unlike

the ^1L_a transition, ^1L_b transition, particularly its spectral shape, is quite sensitive to methyl or methoxy substitution in the indole [16].

For the ^1L_b bands in various solvents, the resolution of the vibronic components and the relative intensities of the 0-0 transitions exhibit significant changes. The 0+2 × 850 transition is almost untraceable for Trp in DMSO (Fig. 4). An assessment was made to determine if there is a relationship between the spectral parameters of Trp (the ^1L_a and ^1L_b bands) and the solvent polarity values.

There is a linear correlation between the spectral parameters of Trp and the solvent polarity values (E_T^N) (Fig. 5). The E_T^N describes the solvent polarity in the vicinity of a solute and takes into account the solvent/solute interaction [31]. Therefore, the E_T^N values more appropriately describe the solvent polarity than, e.g., the dielectric constant or refractive index values, which are macroscopic parameters. It is evident that the parameters obtained in DMSO deviate significantly from the linear correlation curves (Fig. 5). Other than that, the ^1L_a band (λ_{max}) of the Trp absorption spectrum shows positive solvatochromism, i.e., bathochromic shift of the absorption band with increasing solvent polarity. However, in contrast to ^1L_a band, the ^1L_b band (0-0 transition) shows negative solvatochromism, i.e., hypsochromic shift of the absorption band with increasing solvent polarity (Fig. 5A). Similarly, for the Trp derivative, 2,3-dimethylindole, the ^1L_a and ^1L_b bands shift in opposing directions in water from their positions in methylcyclohexane [30]. The position of 0-0 transition of ^1L_b changes minimally in the solvents, despite a large range of the solvent polarity indices (Fig. 5A). Therefore, in proteins, the use of this parameter is limited as an indicator of the local polarity in most cases. However, the relative intensity of the 0-0 transition of the ^1L_b shows sizeable changes in various solvents; there is a linear correlation between the (^1L_b(0-0)/^1L_b(0+850)) parameter and the solvent polarity value (Fig. 5B). The parameter (^1L_b(0-0)/^1L_b(0+850)) determined for Trp in DMSO deviates significantly from the linear correlation curve (Fig. 5B) as seen for other parameters (Fig. 5A).

An assortment of spectral shapes obtained for the ^1L_b band of Trp in various solvents, which may mimic numerous environments in proteins, makes clear that one spectral type of ^1L_b is not sufficient for the spectral fitting of the near-UV CD spectra of the tryptophanyl residues in proteins. Therefore, in the spectral fitting of the near-UV CD spectra of the single tryptophan mutants, each ^1L_b spectrum obtained in various solvents was tested to get the best fit.

The ^1L_b of Trp in DMSO is a result of a specific solvent/solute interaction

It is evident from Figure 4 that compared with other solvents the spectral shape of the ^1L_b of Trp in DMSO is the most altered; the 0+2 × 850 transition of Trp is almost untraceable. In addition, DMSO shifts both the ^1L_a and ^1L_b bands to longer wavelengths relative to their positions in chloroform (Fig. 4). In fact, in DMSO, both bands are the most red shifted. It indicates better stabilization of the indole ring by DMSO molecules in the Franck-Condon excited state relative to the ground state as compared with that of other solvents. The high solvent sensitivity of the ^1L_a state to a solvent polarity has been rationalized by the fact that ^1L_a transition more directly involves the polar nitrogen atom of indole [32]. In addition, the DMSO interaction with Trp leads to the lowest energy for the ^1L_b transition, which does not involve the polar nitrogen atoms of the indole ring. The DMSO-Trp interaction lowers the energy of both the ^1L_a and ^1L_b transitions, which is not the case for the other solvents used in this study. This property of DMSO can be rationalized by its amphiphilic nature. DMSO molecules can be involved in hydrophobic as well as hydrogen bond interactions. The sulfoxide oxygen of DMSO is capable of forming a hydrogen bond with the NH-group of the indole ring. On the other hand, DMSO shows a specific interaction with the Trp residue [33]. It has been shown that the aromatic protons at 2 and 4–7 positions, which are involved in the ^1L_b transition,

exhibit the strongest intermolecular NOE (nuclear Overhauser effect) interactions of the side chain of Trp with DMSO. The result has been interpreted as a hydrophobic interaction between the methyl groups of DMSO and the protons of the indole group [33]. The significant alteration of the ^1L_b band observed for NATA in DMSO shows that the solvent/solute interaction has a dipole-induced dipole and/or van der Waals character (Fig. 4).

A dipolar reaction field will decrease the ^1L_a transition energy if the interaction that localizes the methyl groups of DMSO at the indole ring sets the direction of the dipole moment of DMSO aligned with the $\Delta\mu = \mu_{La} - \mu_g$ (μ_g is the ground-state dipole moment and μ_{La} is the dipole moment of the ^1L_a state. The dipole moment of DMSO is 3.96 D [34] and larger than that of water molecules (1.85 D) [35]. The collective properties of water molecules are responsible for a much larger dielectric constant (~78) compared to that of DMSO (~48). Therefore, DMSO-NATA interaction can lower both the ^1L_a and ^1L_b transition energies. In proteins, it is reasonable to expect a "DMSO-like" ^1L_b band for the tryptophan side chains, when benzene rings of Trp are involved in van der Waals interaction with other side chains.

Resolution of the near-UV CD spectra of F99W in holo- and apo-forms

Analyses of the Trp absorption spectra in various solvents show the disparate nature in the shape of ^1L_b bands, the spectral parameters of which can be linked to the solvent polarity. Each ^1L_b band was tested to achieve the best fit for the near UV-CD spectra of the single-typtophan mutants of TL. The deconvolution of the near-UV CD spectra of F99W (in holo- and apo-forms) and the fitting parameters are shown in Figure 6 and Tables 1 and 2, respectively. It is evident that two different types of the ^1L_b bands are necessary for the spectral fitting of both spectra. Previously, site-directed tryptophan fluorescence (SDTF) studies have revealed that Trp at position 99 exhibits a blue shifted emission peak (λ_{max}= 325 nm) and its side chain is located in a hydrophobic environment inside the cavity of TL [7,8]. Therefore, it is not surprising that the "chloroform-like" ^1L_b band provides the best fit for the CD spectrum of F99W. However, the "methanol-like" ^1L_b band is preferable for the fitting of the CD spectrum of apoF99W. Results of fitting the near-UV CD spectrum of apoF99W with various ^1L_b components show that χ^2/χ^2_{min} values do not differ significantly from each other compared to those for holoF99W or Y87W. The question is whether various types of the ^1L_b band can be accurately discriminated when the range of χ^2/χ^2_{min} values is small. Along with χ^2/χ^2_{min} values, visual inspections of the best fit spectra and their corresponding residuals are very instructive in fitting the near-UV spectrum of apoF99W (Fig. 7 and Fig. 1S, supporting information). Differences at 294.5 nm, 290.7 nm and 285 nm are noticeable for the fitting with the "chloroform-like" ^1L_b band. Particularly, deviations at 290.7 nm and 294.5 nm can be attributed to the fact that the 0-0 band of ^1L_b in chloroform has a smaller width compared with those in methanol or ethanol. Difference absorption spectra of amplitude normalized ^1L_b bands (spectra were also shifted as a whole to match their 0-0 bands to that in methanol) demonstrate deviations in the best fit curve in the above mentioned wavelengths (Fig. 2S, supporting information). The difference between ^1L_b bands is smallest for those of methanol and ethanol. A small difference at 285 nm is noticeable in fitting the apoF99W with an "ethanol like" ^1L_b compared to that of "methanol like". Because spectral parameters of ^1L_b band in methanol and ethanol are very similar, the distinction between them is difficult in proteins.

These results corroborate previous findings. It has been shown that TL undergoes structural and conformational changes upon delipidation. ApoTL exhibits a reduction of β-structure and decreased aromatic side chain asymmetry [27,36]. Compared to the F99W, the fluorescence of apoF99W is red shifted (λ_{max}= 329 nm), which is indicative of a relatively more polar environment [26]. Therefore, the "methanol-like" ^1L_b band found for the apoF99W is consistent with a more polar environment for the position 99 in the apo-protein. The decreased

intensities found for the ^1L_a, ^1L_b of Trp99 as well as total Tyr CD band demonstrate some relaxation of TL structure upon delipidation.

Resolution of the near-UV CD spectra of Y87W. The "DMSO-like" ^1L_b band as a fingerprint for identification of Trp side chain that is involved in van der Waals interaction

The solution and crystal structures of TL have been resolved by SDTF and X-ray crystallography [7,8]. Taking advantage of the available CD spectra of single-tryptophan mutants of TL, we searched the near-UV CD spectra to find an ^1L_b band that is similar to that of Trp in DMSO. The search was narrowed down to the positions at which the benzene ring of indole in the Trp side chain may have a van der Waals interaction with the side chain of a nearest neighbor. As a result, the near-UV CD spectrum of the mutant Y87W and its deconvolution to the components are shown in Figure 8. Only the "DMSO-like" ^1L_b band provides acceptable fitting (Table 1). χ^2/χ^2_{min} values obtained for other type of ^1L_b are >3.4. The decreased total Tyr contribution, which is estimated from of the fitting, is in line with the expected lost contribution of Trp87 (Fig. 1 and 8, Table 2).

Tyr87 is located at the center of the strand F and its side chain points toward the solvent [7, 8]. The energetically favorable rotamer ($g^-(-60°; +90°)$) of Trp87 and the residues in the flanking β-strands are shown in Figure 9. Analysis of the distribution of Trp rotamers in globular proteins show that the rotamer g^- is the most favorable [37,38] in β-strands, particularly at the center of β-strands [38]. It is interesting to note that the estimated contribution of the tryptophan side chain (B_b rotational strength) in the $g^-(-60°; +90°)$ conformation to the far-UV CD is −0.39 DBM (Debye-Bohr magneton, 1 DBM= 0.9273×10^{-38} cgs units) [28], which corroborates the far-UV CD data for the TL mutants. Compared to Y87C, Y87W exhibits a negative contribution (−0.42 DBM) to the far-UV CD (Fig. 2).

One of the factors that stabilize the β-sheet proteins is the interaction between side chains of nearest neighbors [39,40]. Nearest neighbors are divided into two categories: directly hydrogen bonded (HB neighbor) and non-hydrogen bonded (NHB neighbor). Significant side chain-side chain interactions are expected for residues that are NHB neighbors, in which C_α atoms point toward each other, and the C_α-C_α distance is smaller. For the residue Trp87, the HB and NHB neighbors are Tyr100 and Lys 76, respectively. Consequently, interaction between side chains of Trp87 and Lys76 is expected (Fig. 9). Finally, the fluorescence data on β-strand F is an additional argument for the such interaction [7] (Fig. 9, inset). The Trp fluorescence λ_{max} value at position 87 is blue shifted compared with that of flanking positions on the same strand (85 and 89).

Conclusion

A new strategy employs various experimental ^1L_b bands to resolve the near-UV CD spectra of Trp residues into ^1L_a and ^1L_b components. Various types of ^1L_b band can be used to fit the near-UV CD spectra of tryptophanyl residues, the nearest environment of the side chain of which differ significantly from each other. Each type of ^1L_b band (via parameter $^1L_b(0\text{-}0)/^1L_b(0+850)$) used in this study can be linked to a particular polarity value. The most altered ^1L_b band, a "DMSO-like" ^1L_b, may be used as a "fingerprint" for identification the tryptophanyl side chains, in which benzene rings are involved in van der Waals interactions. This study focused mainly on changes in the vibronic bands of the ^1L_b and their correlations with the local environments of Trp side chains in the protein. Other resolved parameters, such as the signs and intensities of the components, the information about the side-chain conformations and dynamics. For TL, dynamic characteristics of the side chains identified from different spectroscopic techniques have been related to differences in intensities of Trp near-UV CD spectra [15]. This method together with Trp mutagenesis, results in site-

directed circular dichroism and complements SDTF studies in extracting conformational as well as structural data of a variety proteins.

Supplementary Material

Refer to Web version on PubMed Central for supplementary material.

Acknowledgements

Supported by U.S. Public Health Service Grants NIH EY 11224 and EY 00331 as well as the Edith and Lew Wasserman Endowed Professorship in Ophthalmology.

References

1. Adams PD, Chen Y, Ma K, Zagorski MG, Sonnichsen FD, McLaughlin ML, Barkley MD. Intramolecular quenching of tryptophan fluorescence by the peptide bond in cyclic hexapeptides. J Am Chem Soc 2002;124:9278–9286. [PubMed: 12149035]
2. Chen Y, Barkley MD. Toward understanding tryptophan fluorescence in proteins. Biochemistry 1998;37:9976–9982. [PubMed: 9665702]
3. McLaughlin ML, Barkley MD. Time-resolved fluorescence of constrained tryptophan derivatives: implications for protein fluorescence. Methods Enzymol 1997;278:190–202. [PubMed: 9170314]
4. Vivian JT, Callis PR. Mechanisms of tryptophan fluorescence shifts in proteins. Biophys J 2001;80:2093–2109. [PubMed: 11325713]
5. Callis PR. 1La and 1Lb transitions of tryptophan: applications of theory and experimental observations to fluorescence of proteins. Methods Enzymol 1997;278:113–150. [PubMed: 9170312]
6. Pan CP, Callis PR, Barkley MD. Dependence of tryptophan emission wavelength on conformation in cyclic hexapeptides. J Phys Chem B 2006;110:7009–7016. [PubMed: 16571015]
7. Gasymov OK, Abduragimov AR, Yusifov TN, Glasgow BJ. Site-directed tryptophan fluorescence reveals the solution structure of tear lipocalin: evidence for features that confer promiscuity in ligand binding. Biochemistry 2001;40:14754–14762. [PubMed: 11732894]
8. Breustedt DA, Korndorfer IP, Redl B, Skerra A. The 1.8-A crystal structure of human tear lipocalin reveals an extended branched cavity with capacity for multiple ligands. J Biol Chem 2005;280:484–493. [PubMed: 15489503]
9. Herskovits TT, Sorensen M. Studies of the location of tyrosyl and tryptophyl residues in protein. II. Applications of model data to solvent perturbation studies of proteins rich in both tyrosine and tryptophan. Biochemistry 1968;7:2533–2542. [PubMed: 4873176]
10. Fasman, GD., editor. Circular dichroism and the conformational analysis of biomolecules. Plenum Press; New York: 1996.
11. Broos J, Tveen-Jensen K, de Waal E, Hesp BH, Jackson JB, Canters GW, Callis PR. The Emitting State of Tryptophan in Proteins with Highly Blue-Shifted Fluorescence. Angew Chem Int Ed Engl 2007;46:5137–5139. [PubMed: 17539030]
12. Strickland EH. Aromatic contributions to circular dichroism spectra of proteins. CRC Crit Rev Biochem 1974;2:113–175. [PubMed: 4591332]
13. Callis PR, Liu T. Quantitative prediction of fluorescence quantum yields for tryptophan in proteins. J Phys Chem B 2004;108:4248–4259.
14. Barth A, Martin SR, Bayley PM. Resolution of Trp near UV CD spectra of calmodulin-domain peptide complexes into the 1La and 1Lb component spectra. Biopolymers 1998;45:493–501. [PubMed: 9577230]
15. Gasymov OK, Abduragimov AR, Yusifov TN, Glasgow BJ. Resolving near-ultraviolet circular dichroism spectra of single trp mutants in tear lipocalin. Anal Biochem 2003;318:300–308. [PubMed: 12814635]
16. Eftink MR, Selvidge LA, Callis PR, Rehms AA. Photophysics of indole derivatives: Experimental resolution of L_a and L_b transitions and comparison with theory. J Phys Chem 1990;94:3469–3479.

17. Glasgow BJ, Heinzmann C, Kojis T, Sparkes RS, Mohandas T, Bateman JB. Assignment of tear lipocalin gene to human chromosome 9q34-9qter. Curr Eye Res 1993;12:1019–1023. [PubMed: 8306712]
18. Redl B, Holzfeind P, Lottspeich F. cDNA cloning and sequencing reveals human tear prealbumin to be a member of the lipophilic-ligand carrier protein superfamily. J Biol Chem 1992;267:20282–20287. [PubMed: 1400345]
19. Glasgow BJ. Tissue expression of lipocalins in human lacrimal and von Ebner's glands: colocalization with lysozyme. Graefes Arch Clin Exp Ophthalmol 1995;233:513–522. [PubMed: 8537027]
20. Cormack, B. Current Protocol in Molecular Biology. Greene Pub. Associates and Wiley-Interscience; New York, N.Y: 1987.
21. Gasymov OK, Abduragimov AR, Yusifov TN, Glasgow BJ. Binding studies of tear lipocalin: the role of the conserved tryptophan in maintaining structure, stability and ligand affinity. Biochim Biophys Acta 1999;1433:307–320. [PubMed: 10515687]
22. Marston, FAO. The Purification of Eukaryotic Polypeptides Expresses in Eschericia coli, The Purification of Eukaryotic Polypeptides Expresses in Eschericia coli. In: Glover, DM., editor. DNA Cloning: a practical approach. IRL Press; Oxford, England: 1987. p. 59-88.
23. Glasgow BJ, Abduragimov AR, Farahbakhsh ZT, Faull KF, Hubbell WL. Tear lipocalins bind a broad array of lipid ligands. Curr Eye Res 1995;14:363–372. [PubMed: 7648862]
24. Bozimowski D, Artiss JD, Zak B. The variable reagent blank: protein determination as a model. J Clin Chem Clin Biochem 1985;23:683–689. [PubMed: 4067517]
25. Strickland EH, Billups C. Oscillator strengths of the 1La and 1Lb absorption bands of tryptophan and several other indoles. Biopolymers 1973;12:1989–1995. [PubMed: 4744748]
26. Gasymov OK, Abduragimov AR, Yusifov TN, Glasgow BJ. Resolution of ligand positions by site-directed tryptophan fluorescence in tear lipocalin. Protein Sci 2000;9:325–331. [PubMed: 10716184]
27. Gasymov OK, Abduragimov AR, Yusifov TN, Glasgow BJ. Structural changes in human tear lipocalins associated with lipid binding. Biochim Biophys Acta 1998;1386:145–156. [PubMed: 9675263]
28. Woody RW. Contributions of tryptophan side chains to the far-ultraviolet circular dichroism of proteins. Eur Biophys J 1994;23:253–262. [PubMed: 7805627]
29. Woody RW. Aromatic side-chain contributions to the far ultraviolet circular dichroism of peptides and proteins. Biopolymers 1978;17:1451–1497.
30. Strickland EH, Billups C, Kay E. Effects of hydrogen bonding and solvents upon the tryptophanyl 1La absorption band. Studies using 2,3-dimethylindole. Biochemistry 1972;11:3657–3662. [PubMed: 5053764]
31. Reichardt C. Solvatochromic dyes as solvent polarity indicators. Chem Rev 1994;94:2319–2358.
32. Lakowicz, JR. Principles of Fluorescence Spectroscopy. 3. Springer; New York: 2006.
33. Angulo M, Hawat C, Hofmann HJ, Berger S. Site-specific solvation determined by intermolecular nuclear Overhauser effect--measurements and molecular dynamics. Org Biomol Chem 2003;1:1049–1052. [PubMed: 12929646]
34. Winsor P, Cole RH. Dlelectrlc properties of electrolyte solutions. 1. Sodium iodide in seven solvents at various temperatures. J Phys Chem 1982;86:2486–2490.
35. Sharma M, Resta R, Car R. Dipolar correlations and the dielectric permittivity of water. Phys Rev Lett 2007;98:247401. [PubMed: 17677991]
36. Glasgow BJ, Abduragimov AR, Yusifov TN, Gasymov OK. Studies of ligand binding and CD analysis with apo- and holo-tear lipocalins. Adv Exp Med Biol 1998;438:105–112. [PubMed: 9634872]
37. Lovell SC, Word JM, Richardson JS, Richardson DC. The penultimate rotamer library. Proteins 2000;40:389–408. [PubMed: 10861930]
38. McGregor MJ, Islam SA, Sternberg MJ. Analysis of the relationship between side-chain conformation and secondary structure in globular proteins. J Mol Biol 1987;198:295–310. [PubMed: 3430610]
39. Minor DL Jr, Kim PS. Context is a major determinant of beta-sheet propensity. Nature 1994;371:264–267. [PubMed: 8078589]

40. Lietzow MA, Hubbell WL. Motion of spin label side chains in cellular retinol-binding protein: correlation with structure and nearest-neighbor interactions in an antiparallel beta-sheet. Biochemistry 2004;43:3137–3151. [PubMed: 15023065]

41. Guex N, Peitsch MC. SWISS-MODEL and the Swiss-PdbViewer: an environment for comparative protein modeling. Electrophoresis 1997;18:2714–2723. [PubMed: 9504803]

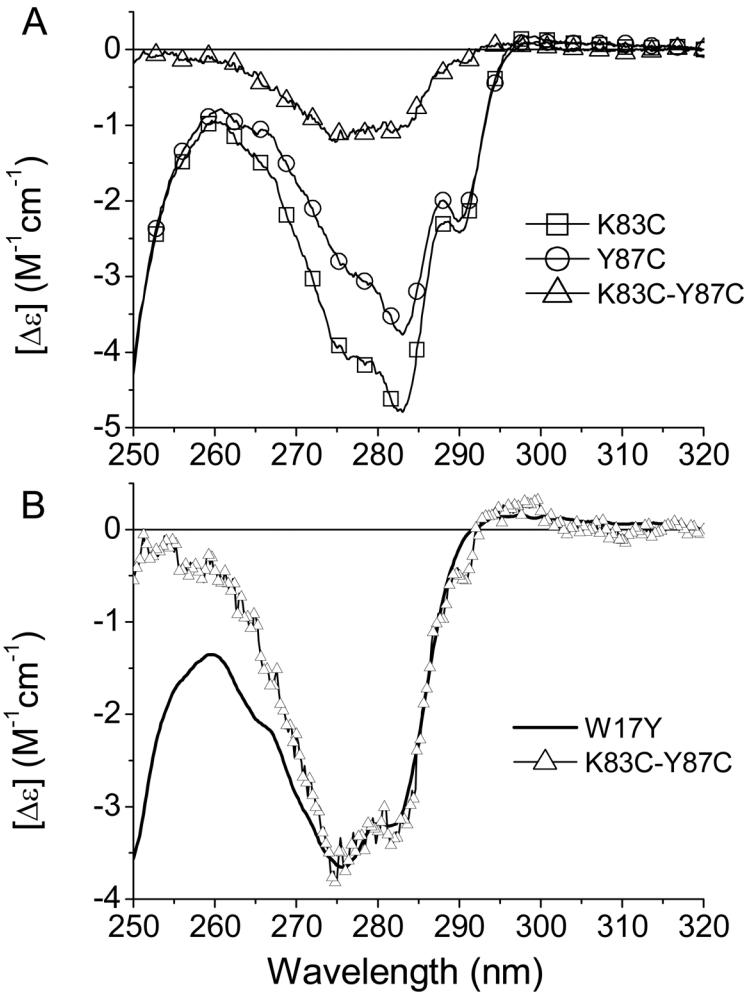

Figure 1.
(A) Near-UV CD spectra of the mutants K83C and Y87C of TL. The difference CD spectrum of the K83C and Y87C shows the contribution of Tyr 87. (B) Comparison of the CD spectra of the mutant W17Y and the difference CD spectrum. For a better view of the similarity of Tyr contributions, the amplitude of the difference CD was normalized to that of W17Y.

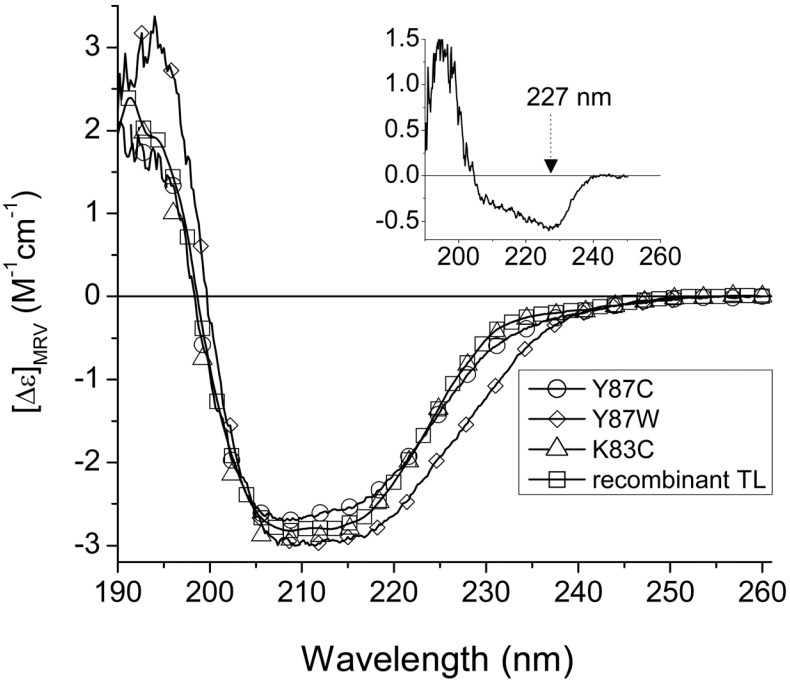

Figure 2.
Far-UV CD spectra of the mutants of TL (K83C, Y87C and Y87W). For comparison, a CD spectrum of the recombinant TL is also shown. The inset shows the difference CD spectrum of the Y87W and Y87C.

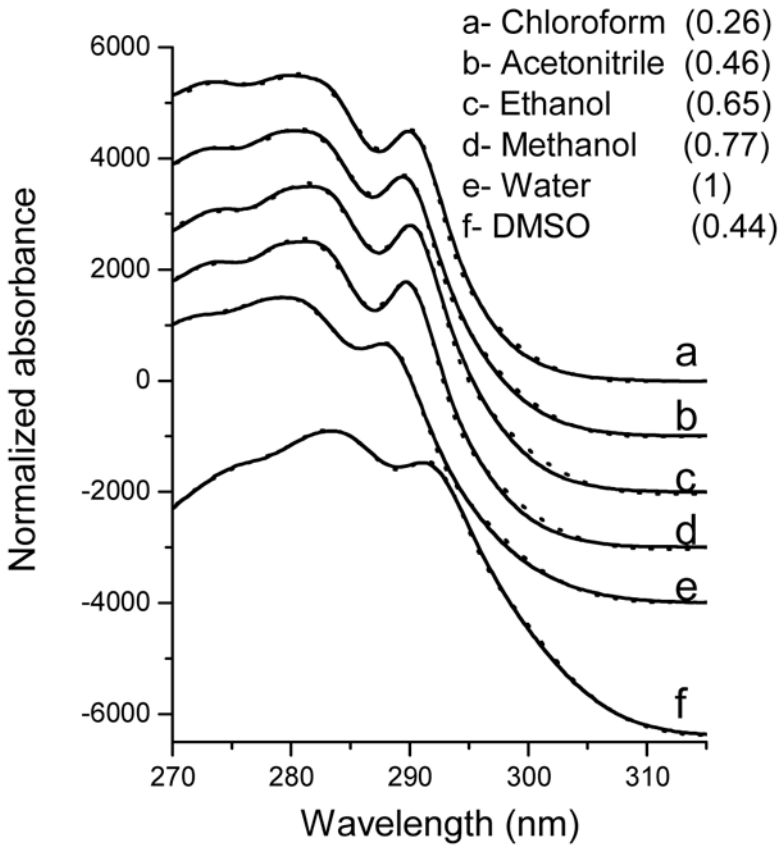

Figure 3.

Absorption spectra (solid curves) of NATA in various solvents. The spectra have been shifted vertically to reduce overlap. The dotted lines are generated by fitting of the experimental data to the sum of the ^1L_a and ^1L_b, spectral (see "Methods" for details) components of which are shown in Figure 4. The numbers in parentheses represent the E_T^N values of corresponding solvents, which were taken from the reference [31].

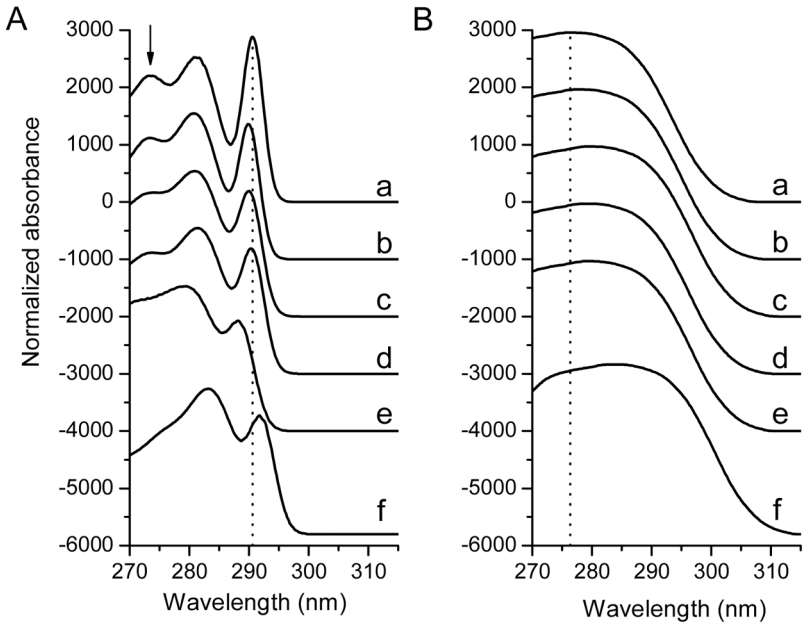

Figure 4.

The resolution of absorption spectra of NATA in various solvents into the ^1L_b (A) and ^1L_a (B) components. Each set of the ^1L_a+^1L_b spectra is the best fit for the absorption spectrum corresponding to the particular solvent (Fig. 3). The spectra have been shifted vertically to reduce overlap. To better follow the solvent-related spectral shift, the dotted vertical lines are located at the 0-0 transition of ^1L_b (A) and the maximum of the ^1L_a bands (B) of NATA in chloroform. The arrow in (A) shows the position of the 0+2×850 transition. The small letters refer to the various solvents (same as in Figure 3).

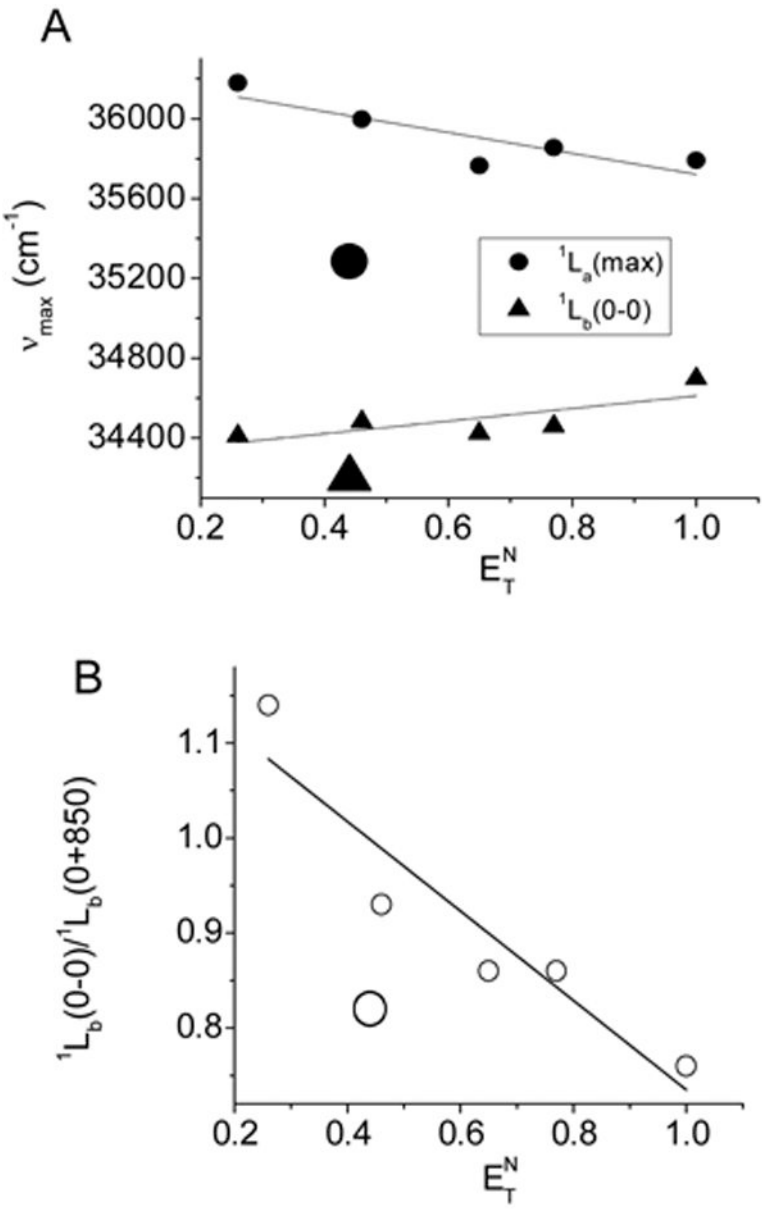

Figure 5.

Linear correlations between solvent polarity values (E_T^N) and the spectral parameters ((A) maxima of the ^1L_a and the 0-0 transition of ^1L_b; (B) ratio of the amplitudes of the 0-0 and 0 +850 transitions) for the absorption spectra of NATA. The positions of the 0-0 transitions of the ^1L_b in various solvents were determined from the 2nd derivative of the corresponding absorption bands. The larger symbols, which are out of the linear correlation, represent the parameters obtained for the absorption spectrum of NATA in DMSO.

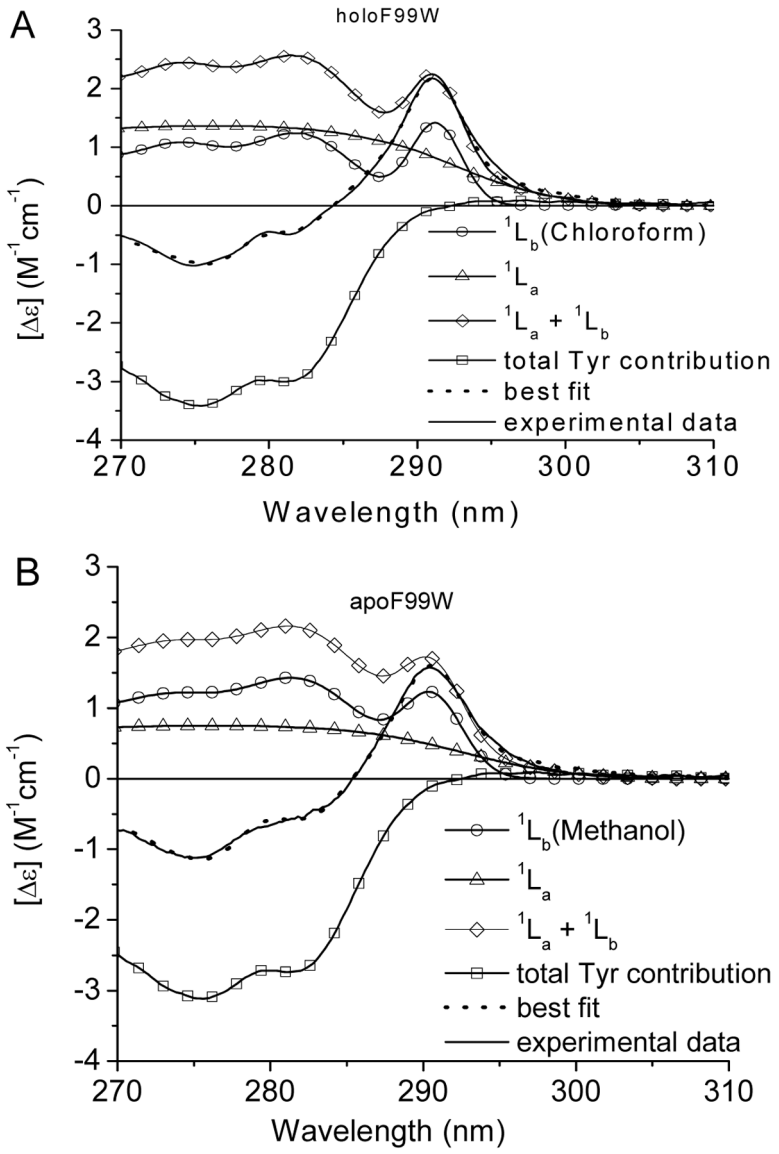

Figure 6.
Fitting of near-UV CD spectra of the tryptophan mutant F99W in holo- (A) and apo-forms (B). Ratios χ^2 values obtained from fitting the CD spectra with the various ^1L_b components are shown in Table 1.

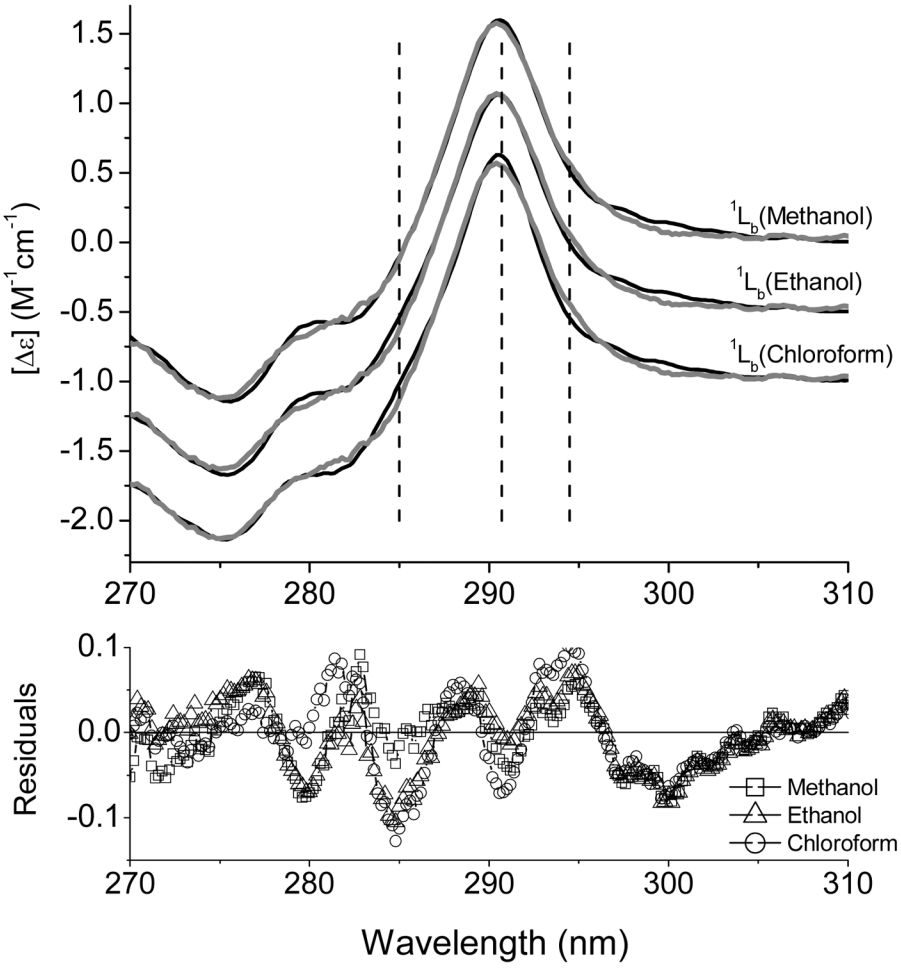

Figure 7.
Fitting for the near-UV CD spectrum of apoF99W with ^1L_b bands obtained in methanol, ethanol and chloroform. Dashed vertical lines correspond to 285 nm, 290.7 nm and 294.5 nm.

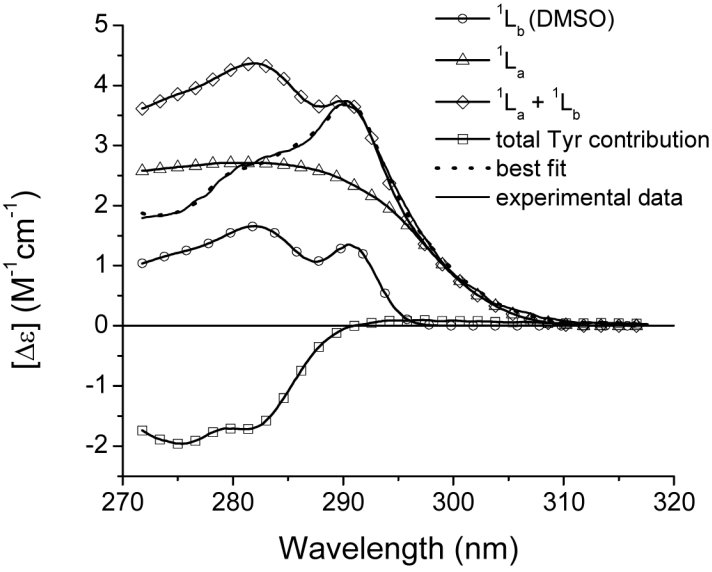

Figure 8.
Fitting of the near-UV CD spectrum of the tryptophan mutant Y87W. Ratios χ^2 values obtained from fitting the CD spectra with the various ^1L_b components are shown in Table 1.

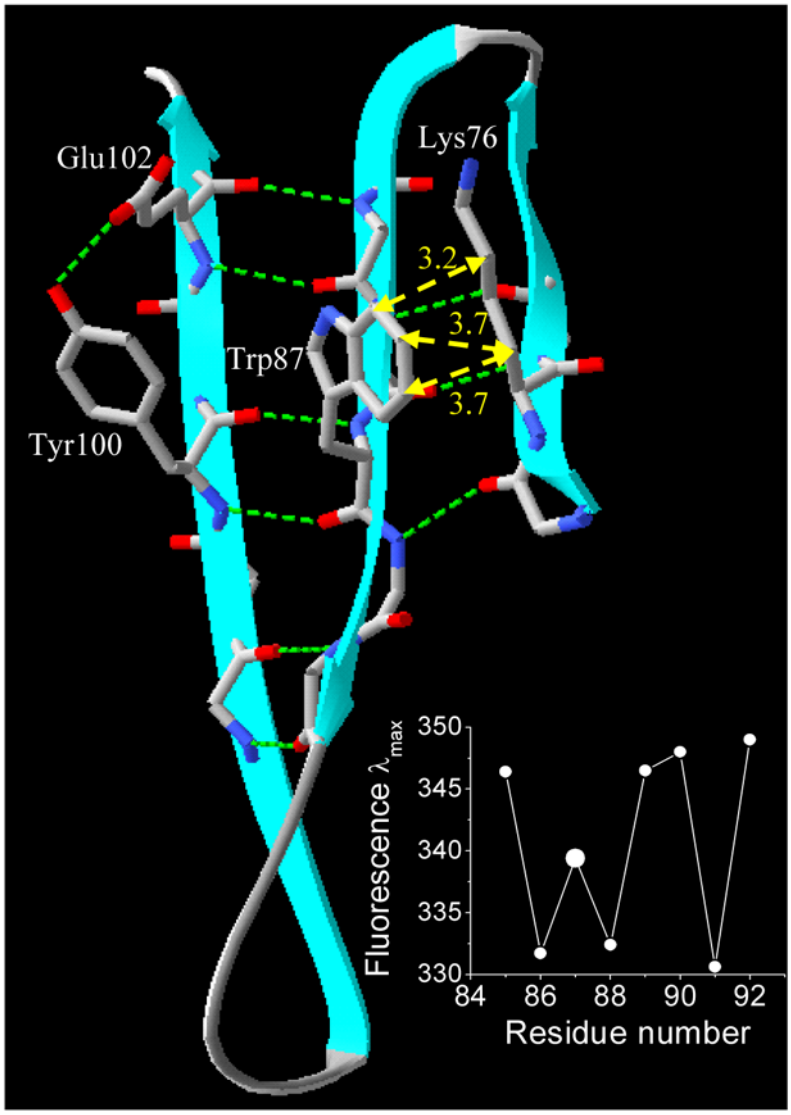

Figure 9.

Ribbon model of TL generated from PDB: 1XKI [8] using SwissPdb Viewer [41]. The position of the side chain of the residue Trp87 (F-strand) relative to that of the residues from flanking strands (Lys76 (E-strand), Tyr100 (G-strand) and Glu102 (G-strand)). The side chains are shown by "stick" representation. Gray, blue and red sticks represent carbon, nitrogen and oxygen atoms, respectively. Dotted green lines show H-bonds. Dotted yellow lines and yellow numbers represent distances (in Å) between the atoms of Trp87 (rotamer $g^{-}(-60°; +90°)$) and Lys76. The inset figure shows the fluorescence λ_{max} values for the single tryptophan mutants in the F-strand [7].

Table 1

Ratios of χ^2 values obtained from the fitting the CD spectra of the single tryptophan mutants with a number of the ^1L_b components corresponding to various solvents

		χ^2/χ^2_{min}	
^1L_b	**F99W**	**apoF99W**	**Y87W**
^1L_b (chloroform)	1	1.42	6.3
^1L_b (ethanol)	1.36	1.08	3.4
^1L_b (methanol)	1.24	1	3.6
^1L_b (acetonitrile)	1.39	1.36	3.8
^1L_b (DMSO)	3.30	1.66	1
^1L_b (water)	1.52	1.12	4.5

Table 2

Resolved parameters for Trp CD spectra in the single Trp mutant proteins of TL.

Mutant	^1L_a		^1L_b		$^1L_{a(max)}/^1L_{b(0-0)}$	W17Y Contribution
	λ_{max} (nm)	Δε of the maximum (M^{-1} cm^{-1})	λ_{max} of (0-0 band) (nm)	Δε of (0-0 band) (M^{-1} cm^{-1})		
F99W	275.7	1.36	291.2	1.42	0.96	0.94
apoF99W	276.0	0.75	290.4	1.23	0.61	0.85
Y87W	280.8	2.71	290.6	1.35	2.01	0.53

Anal Biochem. Author manuscript; available in PMC 2009 March 15.